

Mass-renormalized electronic excitations at $(\pi, 0)$ in the superconducting state of $Bi_2Sr_2CaCu_2O_{8+\delta}$

A. D. Gromko¹, A. V. Fedorov^{1,2}, Y. -D. Chuang^{1,2}, J. D. Koralek¹,

Y. Aiura³, Y. Yamaguchi³, K. Oka³, Yoichi Ando⁴, D. S. Dessau¹

¹*Department of Physics, University of Colorado, Boulder, Colorado 80309-0390*

²*Advanced Light Source, Lawrence Berkeley National Laboratory, Berkeley, CA 94720*

³*National Institute for Advanced Industrial Science and Technology (AIST),*

AIST Tsukuba Central 2, 1-1-1 Umezono, Tsukuba, Ibaraki 305-8568, Japan and

⁴*Central Research Institute of Electric Power Industry (CRIEPI),*

2-11-1 Iwato-Kita, Komae, Tokyo 201-8511, Japan

(Dated: February 5, 2022)

Using high-resolution angle-resolved photoemission spectroscopy on $Bi_2Sr_2CaCu_2O_{8+\delta}$, we have made the first observation of a mass renormalization or "kink" in the E vs. \vec{k} dispersion relation localized near $(\pi, 0)$. Compared to the kink observed along the nodal direction, this new effect is clearly stronger, appears at a lower energy near 40 meV, and is only present in the superconducting state. The kink energy scale defines a cutoff below which well-defined quasiparticle excitations occur. This effect is likely due to coupling to a bosonic excitation, with the most plausible candidate being the magnetic resonance mode observed in inelastic neutron scattering.

PACS numbers: 79.60.Bm, 78.70.Dm

One of the most pressing scientific questions in condensed matter physics concerns the mechanism that binds two electrons into a Cooper pair in high temperature superconductors (HTSCs). It is known that these pairs have d-wave symmetry, with the superconducting gap, $\Delta(\vec{k})$, having a maximum value at the $(\pi, 0)$ point of the two-dimensional Brillouin zone, and zero gap 45° away along the (π, π) line [1, 2]. In conventional superconductors it is known that the s-wave pairing is mediated by the electron-phonon interaction. Most forms of this interaction are isotropic in \vec{k} -space, and are generally unfavorable for the d-wave pairing state found in HTSCs. More likely important for HTSC is a boson that couples strongly to the $(\pi, 0)$ electrons at the d-wave maximum. Here we show direct observations that electrons at $(\pi, 0)$ are strongly coupled to a bosonic excitation, with indications that this boson consists of the famous magnetic resonance mode long observed in inelastic neutron scattering (INS) experiments [3]. We find that this interaction only exists in the superconducting state and is a large effect, strongly renormalizing the E vs. \vec{k} dispersion of the low-energy electronic states.

In the many-body language of solid state physics, the electron self-energy, $\Sigma(\vec{k}, w)$, contains the information of the interactions or correlation effects which "dress" the free electrons in a solid to make quasiparticles. This dressing renormalizes the dispersion of electrons near the Fermi energy, giving them an enhanced mass or flatter E vs. \vec{k} dispersion. At high energies (greater than the energy of the boson being coupled to), the dispersion returns to its bare value, giving the dispersion a "kink". The energy scale and strength of the kink are thus related to the boson energy and coupling strength respectively. Much effort has recently been put forth to study dispersion kinks in relation to HTSC, with the hopes of uncov-

ering the phonons or other bosonic modes which couple to the near- E_F electrons. ARPES is the only direct method for this, with essentially all efforts to date focused on the nodal region of the Brillouin zone [4, 5, 6, 7], where the d-wave superconducting gap goes to zero. Measurements near the $(\pi, 0)$ point of the Brillouin zone, where much of the exotic physics of HTSC such as the maximum in the d-wave superconducting gap [1, 2] and normal state pseudogap [8, 9] occur, have been limited. The main reason for the lack of kink measurements near $(\pi, 0)$ to date are the large widths of spectral features there. While these widths affect the accuracy of determining peak positions, more importantly they can hinder a deconvolution of the bilayer-split bands into their bonding and antibonding components, disallowing measurements of their dispersion. By overdoping high quality single-crystalline $Bi_2Sr_2CaCu_2O_{8+\delta}$ samples, we have obtained very sharp spectral features near $(\pi, 0)$ and for the first time have been able to accurately deconvolve the bilayer splitting as well as superstructure effects [10, 11] with similar work done by Feng et al. [12]. The ability to clearly resolve these separate features is one of the key steps that enabled the new experiments reported here.

We performed high-resolution ARPES experiments on $Bi_2Sr_2CaCu_2O_{8+\delta}$ (Bi2212) samples over a wide range of oxygen concentrations. Samples are labelled with a convention based on the transition temperature (T_c), i.e. an overdoped (OD) Bi2212 sample with $T_c = 58K$ is referred to as OD58. The same convention is used for optimal (OP) and underdoped (UD) samples. All ARPES measurements were taken at beamline 10.0.1 of the Advanced Light Source, Berkeley, and at beamline 5-4 of the Stanford Synchrotron Radiation Laboratory using SES 200 electron spectrometers. The experiments were done using 20eV photons, with a combined experimental energy resolution of 12meV, and a momentum resolution

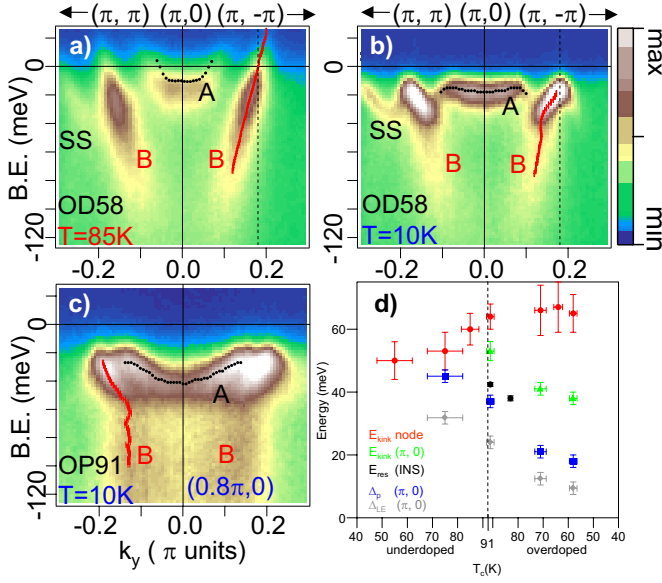


FIG. 1: (a) Normal and (b) superconducting state ARPES data from sample OD58, showing dispersion of the bilayer-split bonding (B) and antibonding (A) bands along the $(\pi, -\pi) - (\pi, 0) - (\pi, \pi)$ symmetry line (see figure 3(e)). (c) Superconducting state data taken on sample OP91, along $(0.8\pi, -\pi) - (0.8\pi, 0) - (0.8\pi, \pi)$. (d) A summary of the energy scales of the ARPES kinks and the INS resonance, for both underdoped (left) and overdoped (right) samples. $E_{\text{kink}}(\text{node})$ is from our own unpublished data [24] and $E_{\text{res}}(\text{INS})$ is from ref. [17].

better than $0.01\pi/a$ (where a is the Bi2212 lattice constant) along the entrance slit to the spectrometer.

Figures 1(a)-(c) show raw data near the $(\pi, 0)$ region (see figure 3(e)) taken on samples OD58 and OP91. A salient feature of the data is the clear resolution of two bands, the higher binding energy bonding band (B) and the lower binding energy antibonding band (A), plus some weak superstructure bands (SS) due to the extra periodicity induced by the Bi-O plane lattice mismatch. Superimposed on top of the B band we show the peak positions (red) determined from Lorentzian fitting of Momentum Distribution Curves (MDCs), which are cuts in momentum space at constant energy. For this data the MDCs display a simple Lorentzian lineshape, allowing us to accurately determine the dispersion. Error bars from the fits are included, but are so small that they are essentially invisible. We also include the dispersion of the A band (black dots), extracted from the sharp low-energy peak in the Energy Distribution Curves (EDCs). The normal state dispersion shown in panel (a) is seen to be nearly linear and featureless in the energy range displayed. Upon cooling the sample to 10K (panel (b)), the dispersion as well as near- E_F spectral weight are radically changed. First, the features do not reach E_F because of the opening of the superconducting gap Δ . In addition to the gap opening, there is a clear kink in the dispersion around 40 meV. Although for sample OP91

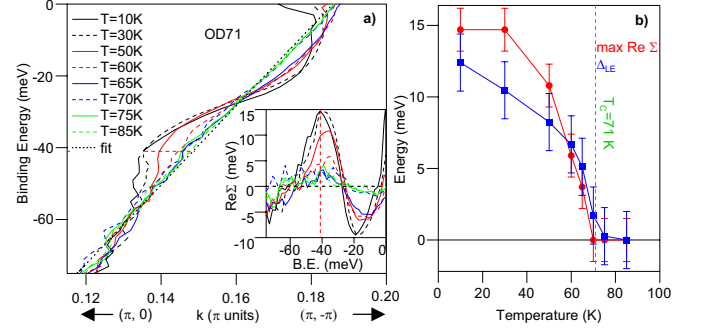


FIG. 2: (a) The MDC bonding-band dispersion from sample OD71 along $(\pi, 0) - (\pi, -\pi)$. The black dotted line is a linear fit to the $T = 85K$ curve. The inset to panel (a) shows the temperature dependence of $Re\Sigma$ determined using the linear fit. The red dashed line indicates the kink energy of $\approx 40meV$. (b) The temperature dependence of the maximum in $Re\Sigma$ (red circles) and the superconducting gap $\Delta_{LE}(T)$ (blue squares).

the spectral features are broader due to decreased doping (panel (c)), the data show a similar effect.

The temperature dependence of the $(\pi, 0)$ kink can be seen in figure 2(a), where the MDC-derived bonding band dispersion from sample OD71 is shown at a series of temperatures taken on cooling through T_c . The black dotted line is a linear fit to the highest temperature ($T = 85K$) data. Since this dispersion is featureless, it is considered to be the non-interacting dispersion. A kink near 40 meV opens up as the temperature is lowered, in addition to low energy changes that are associated with the opening of the superconducting gap [13]. To highlight the temperature dependent effects we subtract the normal state dispersion, shown in the inset to panel (a). In this way we extract $Re\Sigma$ from the data. Panel (b) shows the maximum point of each $Re\Sigma$ curve from the inset in panel (a) as a function of temperature (red), which is seen to have an onset at or very near $T_c = 71K$. In addition, we also plot the superconducting gap Δ_{LE} as a function of temperature (blue) extracted from the identical data set by simply measuring the shift of the midpoint of the EDC leading edge from E_F . We plot $\Delta_{LE}(T)$ in lieu of the gap $\Delta_p(T)$, determined from EDC peak positions, because a reliable determination of $\Delta_p(T)$ is made difficult by thermal broadening. We see that the maximum in $Re\Sigma$, which provides a measure of the coupling strength, tracks the opening of the superconducting gap, making it clear that the two are closely linked.

One may imagine that the $(\pi, 0)$ kink is a byproduct of the opening of the superconducting gap. In particular, if we consider damping of the system due to electron-hole excitations, then each branch will see a turn on at the gap energy Δ , leading to a step in the damping rate $Im\Sigma$ near an energy 3Δ . This will in turn introduce structure into $Re\Sigma$ (as seen by a Kramers-Krönig analysis), and could be imagined as the origin of the kink.

This is somewhat attractive because the temperature as well as \vec{k} -space dependence to first order appear reasonable - it should turn on at T_c and the d-wave nature of Δ may cause some localization of the effect near $(\pi, 0)$. However, as the temperature is raised towards T_c , the energy of the kink is observed to decrease slowly, staying at a sizeable finite value (figure 2(a)). In contrast, the 3Δ model would predict that the kink energy should decrease to zero at T_c , just as Δ does [14].

Figures 3(a)-(d) show the \vec{k} -dependence of the ARPES kink, measured on sample OD71. Data were taken at four momentum slices parallel to the standard $(\pi, 0)$ cuts of figures 1(a)-(b), centered around the \vec{k} values of $(\pi, 0)$, $(0.9\pi, 0)$, $(0.8\pi, 0)$, and $(0.7\pi, 0)$ (blue bars, panel (e)). Panels (a)-(d) show the MDC dispersion of the bonding band from portions of these cuts in both the normal (red) and superconducting (blue) states. From the progression we see that the kink weakens dramatically as we move away from the $(\pi, 0)$ point, such that it is barely visible in the 0.7π cut of panel (d).

There is another key physical property discussed in the HTSC literature that has a similar temperature and momentum dependence as the kink, namely the magnetic resonance mode observed in inelastic neutron scattering (INS) experiments. The resonance mode only occurs below T_c [15], or in underdoped samples below T^* [16]. It has a characteristic energy near 40meV for optimally doped samples and is centered at a wavevector $\vec{Q} = (\pi, \pi)$. The open black circles of figure 4(f) show the resonance mode intensity as a function of momentum transfer \vec{Q} for an OD83 Bi2212 sample, extracted from the INS studies of He et al. [17]. The mode half-intensity points are at approximately $\vec{Q} = 0.66(\pi, \pi)$ and $1.33(\pi, \pi)$ along this cut (green dashed lines, panel (f)), and are expected to be roughly isotropic in \vec{Q} -space [18]. We show these half-intensity points schematically on the Brillouin zone in panel (e) as green circles centered around $(\pi, 0)$ and $(0, \pi)$, according to the standard belief that the (π, π) mode connects these points since they have the largest near- E_F electron density and are separated by a vector of (π, π) [19]. The circles are drawn so that the closest (furthest) edges are connected by a \vec{Q} of $0.66(\pi, \pi)$ ($1.33(\pi, \pi)$). In this way, if we were to plot circles representative of the endpoints of the bottom axis in panel (f), these circles would just touch each other.

We converted the \vec{k} -space values of the Fermi surface crossing locations (panel (e), blue dots) into a radial \vec{k} -distance from the $(\pi, 0)$ points in units of $\sqrt{2}\pi$, listed in panels (a) - (d). The top axis of panel (f) shows the maximum in $Re\Sigma$ plotted versus radial distance from $(\pi, 0)$, with the edges of the plot again corresponding to the situation where circles centered at $(\pi, 0)$ just touch. Since we do not have kink data exactly at the $(\pi, 0)$ point, we scale the vertical axes to match for the $(\pi, 0.19\pi)$ point. The excellent agreement between the neutron and ARPES intensities makes an intimate relationship between the kink

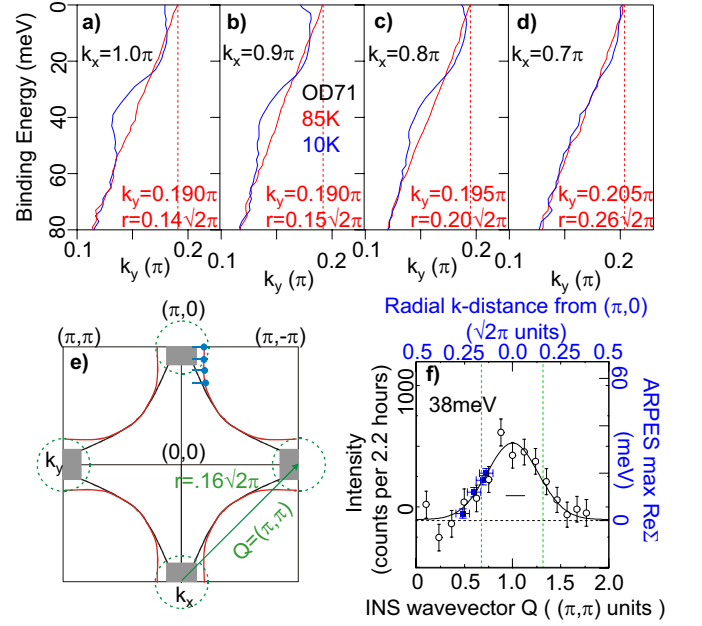


FIG. 3: (a)-(d) The MDC-derived bonding-band dispersion extracted from momentum cuts on sample OD71 (shown as blue bars in panel (e)), at 85K (red) and 10K (blue). The red dashed lines mark the FS crossing locations, which are also labelled on each panel along with the radial distance from $(\pi, 0)$. (e) The Fermi surface with INS wavevectors (green) connecting the $(\pi, 0)$ and $(0, \pi)$ points. Momentum transfer from the surface of one green circle to another represents the INS half-intensity values. (f) INS intensity vs. \vec{Q} from He et al. (33). Overlaid with this is the maximum in $Re\Sigma$ (blue squares) versus the radial distance from $(\pi, 0)$ (top axis).

and the magnetic mode highly plausible.

The trends in the ARPES spectral weight also support the notion of coupling to a boson such as the magnetic mode. In particular, the superconducting state ARPES peaks are seen to be sharp and intense for binding energies below the kink energy (figure 1(b)), whereas they are strongly damped for binding energies above the kink energy, as well as for all energies in the normal state (figure 1(a)). This is expected within the bosonic coupling picture because at low energies, only virtual excitations of the boson are present, which renormalize the electronic excitations. At high energies, real excitations of the boson will be allowed, causing a rapid turn-on of the damping effect. The peak broadening in the normal state, which is believed to represent its "non-quasiparticle-like" nature, has also received intense attention [20, 21, 22]. Interestingly, at high binding energies (100 meV and above), the spectral weight is essentially identical in the normal and superconducting states. A possible explanation for this is that above T_c the magnetic excitations are greatly smeared out in energy but retain a similar \vec{Q} -dependence, as neutron data is beginning to show [23].

From the above data, the differences between the $(\pi, 0)$ kink and the well-studied nodal kink can be summarized

as follows: 1) The $(\pi, 0)$ kink strength is strongly temperature dependent (figure 2), while the nodal kink is roughly temperature independent [6, 7]. 2) The $(\pi, 0)$ kink is at a significantly lower energy scale than the nodal kink (figure 1(d)) and has a different momentum dependence. 3) The strength of the $(\pi, 0)$ kink (or coupling strength) is much stronger than the nodal kink [24]. These points make a strong case that the two kinks are separate entities. The very strong temperature dependence of the $(\pi, 0)$ kink, as well as the tight localization of the kink in k-space make it unlikely that electron-phonon coupling is responsible for the $(\pi, 0)$ kink, although it does remain a possibility for the nodal kink [6]. Another possibility for the origin of the nodal kink is coupling to the local magnetic susceptibility, which is observed in \vec{Q} -integrated INS measurements and which occurs with a slightly higher energy than the magnetic resonance mode [3].

Figure 1(d) shows a comparison of the energy scales of the ARPES kink at $(\pi, 0)$ (green triangles), the INS resonance [17] (black circles), and the nodal kink from our own data [24] (red circles). Following the analogy of $\alpha^2 F(\omega)$ oscillations in strongly electron-phonon coupled conventional s-wave superconductors, we may expect the $(\pi, 0)$ kink to be observed at an energy equal to $\Delta + \omega_R$, where Δ is the superconducting gap and ω_R is the neutron resonance mode energy. In the presence of a varying d-wave gap with a broadened edge, there is no a-priori portion of the gap or gap-edge from which to reference the mode energy. If we choose the superconducting state EDC peak position Δ_p at $(\pi, 0)$ (blue squares), the energies $\Delta_p + \omega_R$ will clearly be larger than the kink energy scale, though if we choose the leading edge half-maximum point Δ_{LE} at $(\pi, 0)$ (gray diamonds), the agreement between $\Delta_{LE} + \omega_R$ and the kink energy scale is much better. Regardless of whether this should be considered an agreement of energy scales, it is not surprising that the situation should be more complicated in the cuprates than in conventional superconductors. For one, the resonance mode to which the electrons appear to be coupling is

not yet understood, even at the basic level of whether it corresponds to particle-particle [25] or particle-hole [26] excitations.

Since the magnetic mode is electronic in origin and only occurs in the paired state, there is a likelihood of a strong feedback effect that may change the observed energy scale. This contrasts with the traditional electron-phonon coupling system, where lattice dynamics are minimally affected by the onset of pairing correlations. In some limits, the energy scale of electronic coupling to the magnetic mode may be similar to the 3Δ case discussed earlier [27], as the magnetic mode is often considered to be an electron-hole excitation, albeit one with highly defined constraints in momentum. Finally, we note that the strong coupling near the $(\pi, 0)$ point makes vertex corrections much more important [28], and these as well as the possibility of excitonic effects [27] may lower the energy of the kink.

In conclusion, we have made the first observation of a kink in the ARPES spectra of HTSC cuprates near the critical $(\pi, 0)$ point of the zone, where the pairing is strongest. The temperature and \vec{k} -dependence of this kink suggest it originates from strong coupling of electrons to the collective magnetic resonance mode long observed in inelastic neutron scattering experiments. This increases the possibility that the magnetic mode acts as the "glue" that couples the electrons together within a Cooper pair.

We acknowledge sample preparation help from M. Varney, beamline support from X.J. Zhou, P. Bogdanov, Z. Hussain and D.H. Liu, and helpful discussions with G. Aeppli, A. Chubukov, C. Kendziora, A. Millis, P. Lee, D. Pines, D. Scalapino, J. Schmalian, Z-X. Shen, and S.C. Zhang. We gratefully acknowledge the help of R. Goldfarb at NIST for the use of the SQUID magnetometer. This work was supported by the NSF Career-DMR-9985492 and the DOE DE-FG03-00ER45809. ALS and SSRL are operated by the DOE, Office of Basic Energy Sciences.

-
- [1] Z.-X. Shen *et al.*, Phys. Rev. Lett. **70**, 1553 (1993).
 - [2] C.C. Tsuei and J.R. Kirtley, Phys. Rev. Lett. **85**, 182 (2000).
 - [3] P. Bourges, in *The Gap Symmetry and Fluctuations in High Temperature Superconductors*, edited by J. Bok, B. Deutscher, and D. Pavuna (Plenum Press, Cambridge, 1998).
 - [4] P.V. Bogdanov *et al.*, Phys. Rev. Lett. **85**, 2581 (2000).
 - [5] A. Kaminski *et al.*, Phys. Rev. Lett. **86**, 1070 (2001).
 - [6] A. Lanzara *et al.*, Nature **412**, 510 (2001).
 - [7] P.D. Johnson *et al.*, Phys. Rev. Lett. **87**, 177007 (2001).
 - [8] H. Ding *et al.*, Nature **382**, 51 (1996).
 - [9] A.G. Loeser *et al.*, Science **273**, 325 (1996).
 - [10] Y.-D. Chuang *et al.*, Phys. Rev. Lett. **87**, 177002 (2001).
 - [11] Y.-D. Chuang *et al.*, <http://xxx.lanl.gov/abs/cond-mat/0107002>.
 - [12] D.L. Feng *et al.*, Phys. Rev. Lett. **86**, 5550 (2001).
 - [13] An artifact of the MDC analysis is that inside the gap region ($\approx 0 - 25\text{meV}$), where there is no real quasiparticle peak, the MDC method finds a peak due to the finite energy width of the spectra. We thus focus on the energy range between 25 and 75 meV, where the kink near 40 meV shows a continuous evolution as a function of temperature.
 - [14] In underdoped samples the gap may remain finite up to and across T_c , a phenomenon not found in overdoped samples.
 - [15] H.F. Fong *et al.*, Nature **398**, 588 (1999).
 - [16] P. Dai *et al.*, Science **284**, 1344 (1999).
 - [17] H. He *et al.*, Phys. Rev. Lett. **86**, 1610 (2001).

- [18] H.A. Mook *et al.*, Nature **580**, 580 (1998).
- [19] L.B. Ioffe and A.J. Millis, Phys. Rev. B **58**, 11631 (1998).
- [20] R.B. Laughlin, Advances in Physics **47**, 943 (1999).
- [21] Z.-X. Shen and J.R. Schrieffer, Phys. Rev. Lett. **78**, 1771 (1997).
- [22] G.A. Sawatzky, Nature **342**, 480 (1989).
- [23] P. Bourges *et al.*, Nature **288**, 1234 (2000).
- [24] A.D. Gromko, unpublished.
- [25] E. Demler and S.-C. Zhang, Phys. Rev. Lett. **75**, 4126 (1995).
- [26] M. Eschrig and M.R. Norman, Phys. Rev. Lett. **85**, 3261 (2000).
- [27] A. Abanov, A.V. Chubukov, and J. Schmalian, J. Electron Spectrosc. Relat. Phenom. **117-118**, 129 (2000).
- [28] S.-C. Zhang, private communication.